Mineralogical Magazine (2022), 1–7
doi:10.1180/mgm.2022.61

CAMBRIDGE UNIVERSITY PRESS

Article

Tennantite-(Cd), $Cu_6(Cu_4Cd_2)As_4S_{13}$, from the Berenguela mining district, Bolivia: the first Cd-member of the tetrahedrite group

Cristian Biagioni[1]*, Anatoly Kasatkin[2], Jiří Sejkora[3], Fabrizio Nestola[4] and Radek Škoda[5]

[1]Dipartimento di Scienze della Terra, Università di Pisa, Via Santa Maria 53, 56126 Pisa, Italy; [2]Fersman Mineralogical Museum of the Russian Academy of Sciences, Leninsky Prospekt 18-2, 119071 Moscow, Russia; [3]Department of Mineralogy and Petrology, National Museum, Cirkusová 1740, 193 00, Praha 9, Czech Republic; [4]Dipartimento di Geoscienze, Università di Padova, Via Gradenigo 6, I–35131 Padova, Italy; and [5]Department of Geological Sciences, Faculty of Science, Masaryk University, Kotlářská 2, 611 37, Brno, Czech Republic

Abstract

Tennantite-(Cd), $Cu_{10}Cd_2As_4S_{13}$, was approved as a new mineral species from the Berenguela mining district, Pacajes Province, La Paz, Bolivia. It occurs as black metallic anhedral grains, up to 1 mm across, associated with baryte, montmorillonite and secondary Cd-sulfates (aldridgeite, niedermayrite and voudourisite). In reflected light, tennantite-(Cd) is isotropic and grey with brownish tints. Reflectance data for the four COM wavelengths in air are [λ (nm): *R* (%)]: 470: 30.0; 546: 30.1; 589: 28.2; and 650: 25.8. Electron microprobe analysis gave (in wt.% – average of 11 spot analyses): Cu 40.56(32), Ag 0.05(5), Fe 0.04(1), Zn 1.91(63), Cd 11.32(1.09), Hg 0.04(7), As 19.04(43), S 26.78(30), total 99.74(53). On the basis of $\Sigma Me = 16$ atoms per formula unit (apfu), the empirical formula of tennantite-(Cd) is $Cu_{9.98}Ag_{0.01}Cd_{1.57}Zn_{0.46}Fe_{0.01}As_{3.97}S_{13.05}$. Tennantite-(Cd) is cubic, $I\bar{4}3m$, with unit-cell parameters $a = 10.3088(2)$ Å, $V = 1095.53(6)$ Å^3 and $Z = 2$. Its crystal structure was refined by single-crystal X-ray diffraction data to a final $R_1 = 0.0152$ on the basis of 359 unique reflections with $F_o > 4\sigma(F_o)$ and 22 refined parameters. Tennantite-(Cd) is isotypic with other tetrahedrite-group minerals. Its crystal-chemistry is discussed and previous findings of Cd-rich tetrahedrite-group minerals are briefly reviewed.

Keywords: tennantite-(Cd), new mineral, sulfosalt, copper, cadmium, arsenic, crystal structure, Berenguela mining district, Bolivia

(Received 29 April 2022; accepted 27 June 2022; Accepted Manuscript published online: 13 July 2022; Associate Editor: G. Diego Gatta)

Introduction

Cadmium ($Z = 48$) belongs to Group 12 of the periodic table and is similar to Zn ($Z = 30$) and Hg ($Z = 80$) in its chemical and physical properties. Abundances of Cd, Zn and Hg in the upper continental crust are 0.102, 52 and 0.056 μg/g, respectively (Wedepohl, 1995). Owing to its chalcophile behaviour, Cd is hosted mainly in sulfides and usually replaces Zn in sphalerite and other Zn-bearing chalcogenides. Currently, only 28 minerals contain Cd as a species-forming element, and the most represented crystal-chemical classes are those of sulfides and sulfosalts (11 species), sulfates (7), and phosphates and arsenates (6). Cadmium chalcogenide minerals are given in Table 1. Among them, the most common minerals are the two dimorphs of the CdS compound, greenockite (wurtzite-type) and hawleyite (sphalerite-type); they usually occur in hydrothermal environments as well as in coatings on sphalerite. Tennantite-(Cd) is the last addition to this group of Cd-bearing compounds.

The examination of an old specimen from the Berenguela mining district, Pacajes Province, La Paz, Bolivia, originally belonging to an old German collection, led to the recognition of a new potential Cd-member of the tennantite series. Further chemical and crystallographic investigations confirmed such a preliminary identification, allowing the proposal of the new mineral species tennantite-(Cd). The new mineral and its name, in keeping with the current nomenclature of tetrahedrite group (Biagioni *et al.*, 2020a), have been approved by the Commission on New Minerals, Nomenclature and Classification of the International Mineralogical Association, under the voting number 2021-083 (Biagioni *et al.*, 2022b). Its mineral symbol, in accord with Warr (2021), is Tnt-Cd. The holotype specimen is deposited in the collections of the Fersman Mineralogical Museum of the Russian Academy of Sciences, Moscow, Russia, under catalogue number 97773. Cotype material is kept in the collections of the Department of Mineralogy and Petrology, National Museum in Prague, Cirkusová 1740, 193 00 Praha 9, Czech Republic, with registration number P1P 47/2021.

In this paper the description of tennantite-(Cd) is reported.

Occurrence and physical properties

Tennantite-(Cd) was found on a specimen from the Berenguela mining district, which is located ~35 km north-east of where the borders of Chile, Peru and Bolivia intersect, at the headwaters of the Rio Berenguela (Fig. 1). The mining district includes several sediment- and volcanic-hosted veins that were exploited during Spanish colonial times. No mining activity has taken place since

*Author for correspondence: Cristian Biagioni, Email: cristian.biagioni@unipi.it
Cite this article: Biagioni C., Kasatkin A., Sejkora J., Nestola F. and Škoda R. (2022) Tennantite-(Cd), $Cu_6(Cu_4Cd_2)As_4S_{13}$, from the Berenguela mining district, Bolivia: the first Cd-member of the tetrahedrite group. *Mineralogical Magazine* 1–7. https://doi.org/10.1180/mgm.2022.61

Table 1. Cadmium sulfides and sulfosalts.

Mineral	Chemical formula*	Space group	Main occurrences
Barquillite	$Cu_2(Cd,Fe)GeS_4$	$I\bar{4}2m$	Hydrothermal veins
Cadmoindite	$CdIn_2S_4$	$Fd\bar{3}m$	Volcanic fumaroles
Cadmoselite	CdSe	$P6_3mc$	Hydrothermal veins, sedimentary rocks
Černýite	Cu_2CdSnS_4	$I\bar{4}2m$	Hydrothermal veins, pegmatites
Greenockite	CdS	$P6_3mc$	Widespread in sulfide deposits
Hawleyite	CdS	$F\bar{4}3m$	Widespread in sulfide deposits
Kudriavite	$(Cd,Pb)Bi_2S_4$	$C2/m$	Volcanic fumaroles
Quadratite	$AgCdAsS_3$	$P4_322$	Hydrothermal veins
Ramdohrite	$Pb_{5.9}Fe_{0.1}Mn_{0.1}In_{0.1}Cd_{0.2}Ag_{2.8}Sb_{10.8}S_{24}$	$P2_1/n$	Hydrothermal veins
Tazieffite	$Pb_{20}Cd_2(As,Bi)_{22}S_{50}Cl_{10}$	$C2/c$	Volcanic fumaroles
Tennantite-(Cd)	$Cu_6(Cu_4Cd_2)As_4S_{13}$	$I\bar{4}3m$	Hydrothermal veins

*Chemical formulae after the official IMA-CNMNC List of Mineral Names (http://cnmnc.main.jp/ updated May 2022).

World War II. The rocks of the Berenguela district are divided broadly into Eocene to Oligocene continental sedimentary rocks and Miocene volcanic, volcaniclastic and intrusive rocks. The older sedimentary rocks include the red quartz arenites and mudstones of the Berenguela Formation and black to red arkoses of the Mauri Formation. The Mauri–Berenguela contact is disconformable to uncomformable. The younger volcanic-rich units include interbedded sandstones, conglomerates, reworked tuffaceous sediments and pyroclastic airfall deposits (Wallace, 1975; Jimenez *et al.*, 1993).

The mineral deposits of the Berenguela district include Cd-rich veins in the Berenguela and lower Mauri Formations and Cd-poor veins in the younger volcaniclastic and intrusive rocks. The veins are localised at fracture intersections. The samples containing tennantite-(Cd) were probably mined in the upper part of the veins of the Berenguela Formation in the first half of the 20th century.

Tennantite-(Cd) occurs as anhedral grains, up to 1 × 1 mm in size, black in colour, with a reddish-brown streak, and metallic lustre (Fig. 2). Mohs hardness was not measured, but it should be close to 3½–4, in agreement with other members of the tetrahedrite group. It is brittle, with a conchoidal fracture and indistinct cleavage. Owing to the small amount of available material, density was not measured; on the basis of the empirical formula and the single-crystal X-ray diffraction data, the calculated density is 4.724 g/cm^3. In reflected light, tennantite-(Cd) is isotropic. It is grey, with brownish tints. Internal reflections are very rare, with a brownish-red colour. Reflectance values were measured in air using a spectrophotometer MSP400 Tidas on a Leica microscope, with a 50× objective (Table 2). The reflectance curve for tennantite-(Cd) compared with published data for other

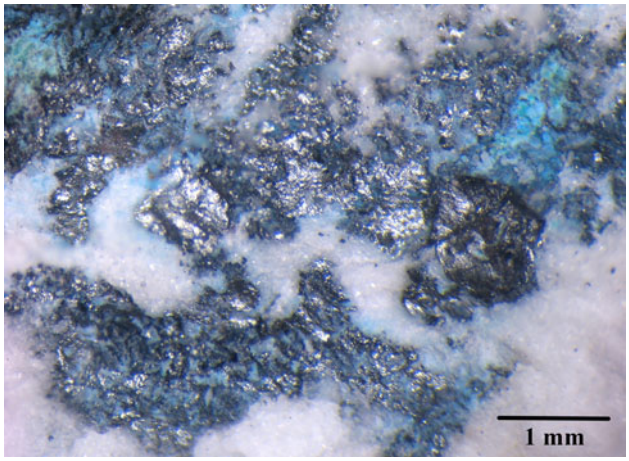

Fig. 2. Tennantite-(Cd), as anhedral grains in baryte with blue aldridgeite. Holotype material (catalogue number 97773).

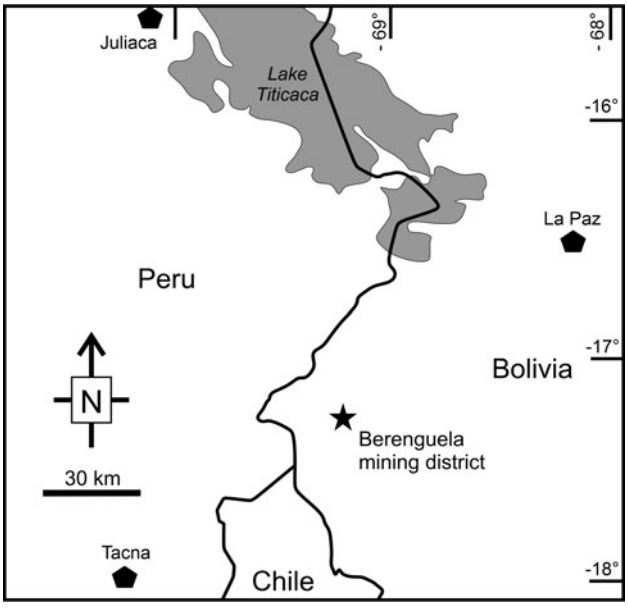

Fig. 1. Location of the Berenguela mining district.

Table 2. Reflectance data for tennantite-(Cd).*

λ (nm)	*R* (%)	λ (nm)	*R* (%)
400	30.9	560	29.6
420	30.6	580	28.7
440	30.2	**589**	**28.2**
460	30.1	600	27.7
470	**30.0**	620	26.8
480	30.0	640	26.1
500	30.1	**650**	**25.8**
520	30.3	660	25.6
540	30.2	680	25.0
546	**30.1**	700	24.6

*The reference wavelengths required by the Commission on Ore Mineralogy (COM) are given in bold.

https://doi.org/10.1180/mgm.2022.61 Published online by Cambridge University Press

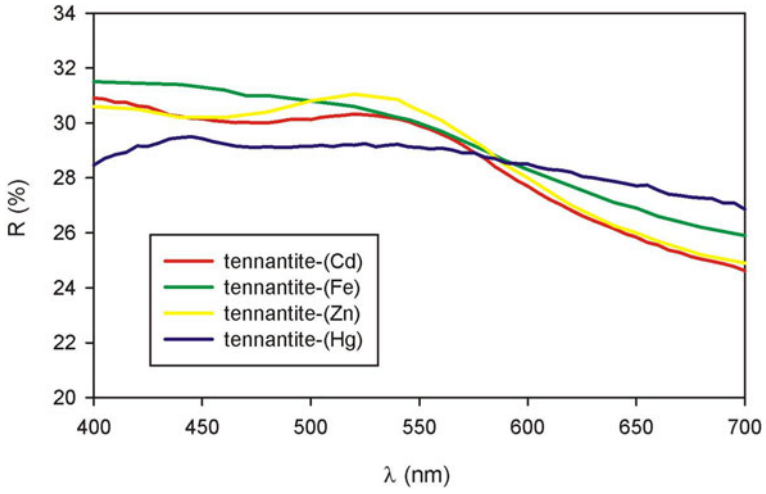

Fig. 3. Reflectance curve for tennantite-(Cd). For the sake of comparison, the reflectance curves of other members of the tennantite series are shown: tennantite-(Fe), Wheal Jewel, Gwennap, Cornwall, U.K. (Criddle and Stanley, 1993); tennantite-(Zn), Tsumeb, Namibia (Criddle and Stanley, 1993); tennantite-(Hg), Lengenbach, Binn Valley, Switzerland (Biagioni *et al.*, 2021).

tennantite-series minerals is shown in Fig. 3. In agreement with Spiridonov *et al.* (1988) for Cd-bearing samples belonging to the tetrahedrite and freibergite series, the reflectance curve of tennantite-(Cd) is similar to that of tennantite-(Zn).

In the holotype specimen, tennantite-(Cd) occurs in baryte, associated with montmorillonite and some Cd-secondary sulfates, i.e. aldridgeite, $(Cd,Ca)(Cu,Zn)_4(SO_4)_2(OH)_6{\cdot}3H_2O$, niedermayrite, $Cu_4Cd(SO_4)_2(OH)_6{\cdot}4H_2O$, and voudourisite, $CdSO_4{\cdot}H_2O$ (Fig. 2).

Chemical data

Quantitative chemical analyses were carried out using a Cameca SX 100 electron microprobe (Department of Geological Sciences, Faculty of Science, Masaryk University, Brno, Czech Republic) and the following experimental conditions: wavelength dispersive spectroscopy mode, accelerating voltage = 25 kV, beam current = 10 nA and beam diameter 2 μm. Standards (element, emission line) were: chalcopyrite (Cu*K*α, S*K*α), Ag (Ag*L*α), FeS_2 (Fe*K*α), ZnS (Zn*K*α), Cd (Cd*L*β), pararammelsbergite (As*L*β) and HgTe (Hg*M*α). The contents of other sought elements with $Z > 8$ (including Sb) were below detection limits. Matrix correction by *PAP* procedure (Pouchou and Pichoir, 1985) was applied to the data. Results are given in Table 3.

X-ray crystallography

Powder X-ray diffraction data (Table 4) were collected at room temperature using a Bruker D8 Advance diffractometer equipped with a solid-state LynxEye detector and secondary monochromator generating Cu*K*α radiation (Department of Mineralogy and Petrology, National Museum, Prague, Czech Republic). The instrument was operating at 40 kV and 40 mA. In order to minimise the background, the powder samples were placed on the surface of a flat Si wafer. The powder diffraction pattern was collected in the Bragg-Brentano geometry in the 2θ range 3–65°, step 0.01°, and counting time of 20 s per step (total duration of the experiment was ~30 hours). The positions and intensities of diffraction lines were found and refined using the Pearson VII profile-shape function of the *ZDS* program package (Ondruš, 1993). Unit-cell parameters were refined using the least-squares software of Burnham (1962) and gave $a = 10.2976(8)$ Å and $V = 1091.9(2)$ Å^3.

Single-crystal X-ray diffraction intensity data were collected using a Supernova Rigaku-Oxford Diffraction single-crystal diffractometer (50 kV and 0.12 mA) equipped with a 200 K Pilatus Dectris detector and graphite-monochromatised Mo*K*α radiation (Dipartimento di Geoscienze, Università di Padova,

Table 3. Chemical data (in wt.%) and atoms per formula unit (apfu), based on Σ*Me* = 16 apfu, for tennantite-(Cd).

Element	wt.%	range (n = 11)	e.s.d.	apfu	range	e.s.d.
Cu	40.56	39.79–40.83	0.32	9.98	9.79–10.13	0.09
Ag	0.05	0.00–0.16	0.05	0.01	0.00–0.02	0.01
Fe	0.04	0.03–0.06	0.01	0.01	0.00–0.02	0.01
Zn	1.91	1.16–2.95	0.63	0.46	0.28–0.70	0.15
Cd	11.32	9.52–12.83	1.09	1.57	1.33–1.78	0.15
Hg	0.04	0.00–0.17	0.07	0.00	0.00–0.01	0.01
As	19.04	18.13–19.59	0.43	3.97	3.85–4.05	0.06
S	26.78	26.32–27.48	0.30	13.05	12.83–13.50	0.19
Total	99.74	98.67–100.45	0.53			

n = number of spot analyses; e.s.d. = estimated standard deviation.

Table 4. Powder X-ray diffraction data for tennantite-(Cd).*

I_{meas}	d_{meas}	d_{calc}	I^1_{calc}	d^1_{calc}	*h k l*
1	7.277	7.281	1	7.289	1 1 0
7	**4.206**	**4.204**	**6**	**4.209**	**2 1 1**
1	3.639	3.641	1	3.645	2 2 0
100	**2.973**	**2.973**	**100**	**2.976**	**2 2 2**
2	2.754	2.725	3	2.755	3 2 1
12	**2.574**	**2.574**	**20**	**2.577**	**4 0 0**
4	2.4281	2.4272	4	2.430	3 3 0
		2.4272	2	2.430	4 1 1
–	–	–	1	2.198	3 3 2
3	2.0193	2.0195	1	2.022	5 1 0
		2.0195	4	2.022	4 3 1
5	1.8808	1.8801	8	1.882	5 2 1
27	**1.8212**	**1.8204**	**43**	**1.822**	**4 4 0**
1	1.7663	1.7660	2	1.768	4 3 3
3	1.6708	1.6705	1	1.672	5 3 2
		1.6705	4	1.672	6 1 1
–	–	–	1	1.630	6 2 0
8	**1.5531**	**1.5524**	**23**	**1.554**	**6 2 2**
2	1.4864	1.4863	3	1.488	4 4 4
1	1.4565	1.4563	1	1.458	7 1 0

*Notes: I^1_{calc}, d^1_{calc} were calculated using the software *PowderCell*2.3 (Kraus and Nolze, 1996) on the basis of the structural model given in Table 6. Only reflections with $I_{calc} > 1$ are listed; the strongest lines are given in bold.

https://doi.org/10.1180/mgm.2022.61 Published online by Cambridge University Press

Table 5. Summary of crystal data and parameters describing data collection and refinement for tennantite-(Cd).

Crystal data	
Crystal size (mm)	0.050 × 0.045 × 0.040
Cell setting, space group	Cubic, $I\bar{4}3m$
a (Å)	10.3088(2)
V (Å^3)	1095.53(6)
Z	2
Data collection and refinement	
Radiation, wavelength (Å)	Mo$K\alpha$, $\lambda = 0.71073$
Temperature (K)	293(2)
$2\theta_{max}$ (°)	63.95
Measured reflections	7444
Unique reflections	379
Reflections with $F_o > 4\sigma(F_o)$	359
R_{int}	0.0336
$R\sigma$	0.0164
Range of h, k, l	$-14 \le h \le 14$, $-14 \le k \le 14$, $-14 \le l \le 15$
R [$F_o > 4\sigma(F_o)$]	0.0152
R (all data)	0.0168
wR (on F_o^2)[1]	0.0315
Goof	1.148
Absolute structure parameter[2]	0.00(2)
Number of least-squares parameters	22
Maximum and minimum residual peak (e^- Å^{-3})	0.36 [at 1.17 Å from X(3)] −0.45 [at 0.55 Å from M(2b)]

[1] $w = 1/[\sigma^2(F_o^2)+(0.0108P)^2+0.6772P]$.
[2] Flack (1983)

Italy). The detector-to-crystal distance was set at 68 mm. Data were collected by 761 frames over 22 runs in 1° slices, with an exposure time of 60 s per frame, and they were corrected for Lorentz, polarisation, and absorption using the software package *Crysalis Pro*3 (version 41.64.113a). The refined unit-cell parameters are $a = 10.3088(2)$ Å, $V = 1095.53(6)$ Å^3; and space group $I\bar{4}3m$. The crystal structure of tennantite-(Cd) was refined using *Shelxl*-2018 (Sheldrick, 2015) starting from the structural model of Johnson and Burnham (1985). The following neutral scattering curves, taken from the *International Tables for Crystallography* (Wilson, 1992), were initially used: Cu *vs* □ at M(2), Cu *vs* Cd at M(1), As at X(3), S at S(1) and S(2) sites. Several cycles of isotropic refinement converged to $R_1 = 0.095$ confirming the correctness of the structural model. The modelling of the racemic twin suggested that the structure had to be inverted. An anisotropic refinement for cations only converged to $R_1 = 0.038$. The M(2) site displayed a relatively large U_{eq} value, suggesting its splitting, in agreement with previous authors (e.g. Andreasen *et al.*, 2008; Welch *et al.*, 2018). After the addition of the split position, found in the difference-Fourier map, the R_1 value was lowered to 0.0242. The site occupancy factors (s.o.f.) at the two split positions M(2a) and M(2b) were constrained to be 1. After several cycles of anisotropic refinement for all the atoms, the R_1 converged to 0.0152 for 359 unique reflections with $F_o > 4\sigma(F_o)$ and 22 refined parameters. Details of the data collection and crystal structure refinement are reported in Table 5. Fractional atomic coordinates and equivalent isotropic displacement parameters are reported in Table 6, whereas Table 7 reports selected bond distances and Table 8 the weighted bond-valence balance calculated according to the bond parameters of Brese and O'Keeffe (1991). The crystallographic information file has been deposited with the Principal Editor of *Mineralogical Magazine* and is available as Supplementary material (see below).

Table 7. Selected bond distances (Å) for tennantite-(Cd).

M(1)–S(1)	×4	2.3698(6)	M(2a)–S(2)		2.2145(11)
			M(2a)–S(1)	×2	2.2380(11)
			<M(2a)–S>		2.230
X(3)–S(1)	×3	2.2651(10)	M(2b)–S(2)		2.377(8)
			M(2b)–S(1)	×2	2.386(8)
			<M(2b)–S>		2.383

Table 8. Weighted bond-valence sums (in valence unit) for tennantite-(Cd).*

Site	M(1)	M(2a)	M(2b)	X(3)	Σanions	Theor.
S(1)	$^{2\times\rightarrow}0.41^{\times4\downarrow}$	$0.30^{\times2\downarrow}$	$^{2\times\rightarrow}0.02^{\times2\downarrow}$	$0.99^{\times3\downarrow}$	2.15	2.00
S(2)		$^{6\times\rightarrow}0.32$	$^{12\times\rightarrow}0.02$		2.16	2.00
Σcations	1.64	0.92	0.06	2.97		
Theor.	1.33	0.84	0.08	3.00		

*Note: left and right superscripts indicate the number of equivalent bonds involving cations and anions, respectively. The following site populations were used: M(2a) = $Cu_{0.84}$; M(2b) = $Cu_{0.08}$; M(1) = $Cu_{0.67}Cd_{0.26}Zn_{0.07}$; X(3) = $As_{1.00}$.

Results and discussions

Chemical formula

There are different approaches to the recalculation of the chemical formula of a tetrahedrite-group mineral; among them, the two better normalisation methods are based on Σ$Me = 16$ atoms per formula unit (apfu) or on the basis of (As + Sb + Te + Bi) = 4 apfu. The former approach assumes that no vacancies occur at the M(2), M(1) and X(3) sites, whereas the latter is based on the negligible variations in the ideal number of cations hosted at the X(3) site, as discussed by Johnson *et al.* (1986).

Table 6. Sites, Wyckoff positions, site occupancy factors (s.o.f.), fractional atom coordinates and equivalent isotropic displacement parameters (Å^2) for tennantite-(Cd).

Site	Wyckoff position	s.o.f.	x/a	y/b	z/c	U_{eq}
M(2a)	12e	$Cu_{0.841(6)}$	0.78518(10)	0	0	0.0380(7)
M(2b)	24g	$Cu_{0.080(3)}$	0.7844(6)	−0.0578(12)	0.0578(12)	0.0380(7)
M(1)	12d	$Cu_{0.805(5)}Cd_{0.195(5)}$	¾	½	0	0.0204(2)
X(3)	8c	$As_{1.00}$	0.74175(5)	0.74175(5)	0.74175(5)	0.01629(17)
S(1)	24g	$S_{1.00}$	0.88181(8)	0.88181(8)	0.64664(10)	0.0183(2)
S(2)	2a	$S_{1.00}$	0	0	0	0.0186(5)

https://doi.org/10.1180/mgm.2022.61 Published online by Cambridge University Press

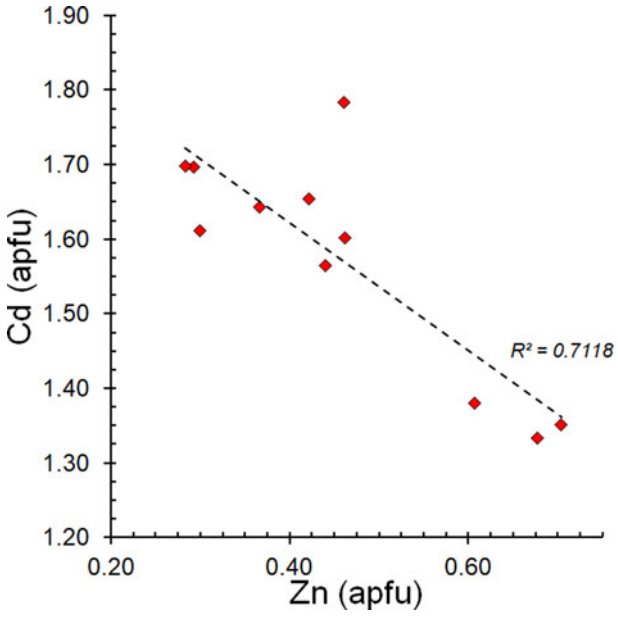

Fig. 4. Relationship between Cd and Zn content (in apfu) in tennantite-(Cd).

The first approach gives the chemical formula $Cu_{9.98(9)}Ag_{0.01(1)}Cd_{1.57(15)}Zn_{0.46(15)}Fe_{0.01(1)}As_{3.97(6)}S_{13.05(19)}$, whereas the other normalisation strategy corresponds to the formula $Cu_{10.04(21)}Ag_{0.01(1)}Cd_{1.59(16)}Zn_{0.46(15)}Fe_{0.01(1)}As_{4.00}S_{13.14(35)}$. The simplified formula of tennantite-(Cd) is $Cu_6Cu_4(Cd,Zn,Fe)_2As_4S_{13}$, corresponding to the end-member formula $Cu_6^+(Cu_4^+Cd_2^{2+})As_4S_{13}$. It corresponds to (in wt.%) Cu 40.30, Cd 14.26, As 19.01, S 26.43, total 100.00.

In the sample studied, the Cu content is very close to the ideal (i.e. 10 apfu), with only a negligible Ag content. The C constituent is represented by Cd and minor Zn; iron, probably occurring as Fe^{3+} (e.g. Makovicky *et al.*, 2003), occurs in very low amounts. Figure 4 shows the Cd *vs*. Zn content in the 11 spot analyses performed on type material; an inverse relation between these two elements is apparent. Finally, chemical data do not support any significant S deficiency in tennantite-(Cd).

Crystal structure description

Tennantite-(Cd) is isotypic with the other members of the tetrahedrite group. Its crystal structure can be described as a framework of corner-sharing $M(1)S(1)_4$ tetrahedra with cavities hosting $X(3)S(1)_3$ pyramids around $S(2)M(2)_6$ octahedra (e.g. Johnson *et al.*, 1988).

The *M*(1) site has a mixed (Cu,Cd,Zn) occupancy. The refined site scattering is 196.2 electrons per formula unit (epfu); this value can be compared with that calculated from the site population proposed on the basis of chemical data, i.e. $^{M(1)}(Cu_{4.00}Cd_{1.55}Zn_{0.45})$, corresponding to 203.9 epfu. The average bond distance is 2.370 Å, longer than that observed in mixed (Cu,Zn/Fe) *M*(1) sites in tetrahedrite-group minerals (e.g. Wuensch, 1964; Wuensch *et al.*, 1966), and similar to the bond distance observed in tetrahedrite-(Hg) and tennantite-(Hg), i.e. 2.3913 Å and 2.389 Å (Biagioni *et al.*, 2020b; 2021), respectively. This agrees with the similar crystal radii of Cd^{2+} and Hg^{2+}, i.e. 0.84 Å (Johnson *et al.*, 1988). Moreover, the ICSD database (Allen *et al.*, 1987) reports structural data of synthetic $Cu_{10}Cd_2Sb_4S_{13}$, based on unit-cell parameters given by Johnson (1991) and refined on the basis of powder X-ray diffraction data. In that structure refinement, the *M*(1)–S(1) distance is 2.367 Å, close to that observed in this work for tennantite-(Cd) from Berenguela.

Note that in the structure of synthetic $Cu_{10}Cd_2Sb_4S_{13}$, Cd is fully attributed to the *M*(2) site. An attempt to refine Cd at both the *M*(2) and *M*(1) sites in tennantite-(Cd) resulted in a slightly worse R_1 factor ($R_1 = 0.0186$). Taking into account the crystal-chemistry of Cd^{2+}, a tetrahedral coordination seems more reasonable (e.g. Borsari, 2014), in agreement with Pattrick (1978), who discussed the replacement of Zn and Fe by Cd in Cd-rich tetrahedrite samples from Scotland, and with Charnock *et al.* (1989), who confirmed the tetrahedral coordination of Cd by extended X-ray absorption fine structure (EXAFS). The bond-valence sum (BVS) at the *M*(1) site is 1.64 valence units (vu), higher than the theoretical value, 1.33 vu (Table 8). Such an over-bonding has been observed in other members of the tetrahedrite group, as in tetrahedrite-(Hg) (1.64 vu) and tennantite-(Hg) (1.68 vu) (Biagioni *et al.*, 2020b; 2021), as well as in tetrahedrite-related phases like arsiccioite (Biagioni *et al.*, 2014). Probably, this discrepancy is due to inaccurate bond parameters for Cd–S bonds. Indeed, using the bond parameters of Brese and O'Keeffe (1991), the following ideal bond distances for tetrahedral coordination can be calculated (in Å): Cu^+ 2.373, Cd^{2+} 2.546 and Zn^{2+} 2.346 Å. Assuming the site population discussed above, the average <*M*(1)–S(1)> bond distance would be 2.416 Å. In greenockite and hawleyite, the observed <Cd–S> distances are 2.528 and 2.526 Å, respectively (Skinner, 1961; Xu and Ching, 1993). Using an average <Cd–S> of 2.527 Å, the calculated *M*(1)–S(1) distance in tennantite-(Cd) would be 2.411 Å, larger than the observed one.

The *M*(2) site is split into two sub-positions, *M*(2a) and *M*(2b), separated by 0.84 Å, whereas the distance between two neighbouring *M*(2b) positions is 1.68 Å. These distances can be compared with those reported in other refinements of the crystal structure of tennantite-series minerals, e.g. in Cu-rich unsubstituted tennantite described by Makovicky *et al.* (2005) or in tennantite-(Cu) (Biagioni *et al.*, 2022a). The *M*(2a) position has a triangular planar coordination, whereas *M*(2b) has a flat trigonal pyramidal one. Average bond distances are 2.230 and 2.383 Å for *M*(2a) and *M*(2b) positions, respectively. A comparison of these distances can be made with those reported in Cu-pure and unsplit *M*(2) sites in tennantite (Wuensch *et al.*, 1966), i.e. 2.240 Å, as well as those in split positions observed in tennantite-(Cu), i.e. 2.230 and 2.307 Å (Biagioni *et al.*, 2022a), and in the Cu-excess tennantite-(Cu) described by Makovicky *et al.* (2005), i.e. 2.217 Å for Cu2A and 2.467 Å for Cu2B. Moreover, the Cu2B of Makovicky *et al.* (2005) is also close to the As site, 2.41 Å, whereas the *M*(2b)–*X*(3) distance is 2.695 Å in the sample from the Berenguela mining district. Probably, the relatively large <*M*(2b)–S> bond distance is due to the average nature of this position. An unconstrained refinement of the s.o.f. at the *M*(2a) and *M*(2b) positions indicated full occupancy of the *M*(2) site by Cu, with no evidence of the possible occurrence of Cu excess or of any other element heavier than Cu (e.g. Cd). The BVS at the *M*(2) site [i.e. *M*(2a) + 2×*M*(2b)] (Table 8) is 1.04 vu, in agreement with the presence of monovalent cations.

The *X*(3) site shows an average bond distance of 2.265 Å, in agreement with its As pure nature; BVS is 2.97 vu (Table 8).

Both S sites were found fully occupied by S; the BVS at the S(1) and S(2) sites are 2.15 and 2.16 vu, respectively.

Coupling the results of the crystal structure refinement and the electron microprobe analysis, the structural formula

https://doi.org/10.1180/mgm.2022.61 Published online by Cambridge University Press

of holotype tennantite-(Cd) can be written as $^{M(2)}Cu_{6.00}{}^{M(1)}(Cu_{4.00}Cd_{1.55}Zn_{0.45})^{X(3)}As_{4.00}{}^{S(1)}S_{12}{}^{S(2)}S$.

Relation between Cd content and unit-cell parameters

The unit-cell parameter *a* of tennantite-(Cd) is ~10.31 Å. Charlat and Lévy (1975) observed that the Zn-to-Fe substitution does not affect the unit-cell parameter of tetrahedrite-group minerals; consequently, the increase of the *a* parameter with respect to that of ideal tennantite-(Fe/Zn), ~10.23 Å, is due to the occurrence of Cd^{2+}.

Pattrick and Hall (1983) observed an increase in the unit-cell parameter of 0.06 Å per Cd atom replacing (Zn/Fe) in synthetic tetrahedrite. Assuming that this relation can be applied to the As-isotype tennantite, the expected unit-cell parameter of the sample studied should be $a \approx 10.32$ Å, in reasonable agreement with the observed one. Johnson *et al.* (1987) proposed the following relation between chemistry and unit-cell parameter (for synthetic tetrahedrites, as no data were available for natural Cd-bearing tetrahedrites): a (Å) = 10.381 + 0.039 Ag + 0.003 Ag^2 − 0.019 Cu* + 0.064 Cd − 0.037 As, where Cu* = [2 − (Fe + Zn + Hg + Cd)]. The calculated unit-cell parameter, assuming the idealised chemical formula $Cu_6[Cu_4(Cd_{1.55}Zn_{0.45})]As_4S_{13}$, is a = 10.33 Å.

Cadmium in tetrahedrite-group minerals

Currently, several members of the tennantite series have been reported: tennantite-(Fe), tennantite-(Zn), tennantite-(Hg), tennantite-(Cu) and tennantite-(Ni) (Biagioni *et al.*, 2020a, 2021, 2022a; Wang *et al.*, 2021). Tennantite-(Cd) is another addition to this series and its occurrence is in keeping with the similar crystal-chemical behaviour of Zn and Cd. Probably, the rarity of Cd-bearing tetrahedrite-group minerals may be related not only to the low Cd abundance but also to its preference to being partitioned in chalcopyrite and sphalerite; indeed Cd contents are higher in those tetrahedrite-group mineral samples crystallising in sphalerite- and chalcopyrite-free assemblages or in unusually Cd-enriched environments (George *et al.*, 2017).

Notwithstanding this rarity, some authors reported the occurrence of Cd-rich tetrahedrite-group minerals. Pattrick *et al.* (1978) found up to 1.92 Cd apfu in samples from Tyndrum, Scotland, UK, whereas Voudouris *et al.* (2011) reported 1.97 Cd apfu from the Evia Island, Greece, and Jia *et al.* (1988) measured 1.85 Cd apfu in a sample from Xitieshan, China. These latter authors actually gave the formula $(Cu_{6.95}Ag_{3.03})_{\Sigma 9.98}(Cd_{1.85}Zn_{0.15}Fe_{0.15})_{\Sigma 2.15}(Sb_{4.19}As_{0.25})_{\Sigma 4.44}S_{13}$; taking into account the partitioning of Ag at the *M*(2) site, this formula could represent an intermediate composition between the hypothetical end-members $Ag_6(Cu_4Cd_2)Sb_4S_{13}$, i.e. 'argentotetrahedrite-(Cd)', and $Cu_6(Cu_4Cd_2)Sb_4S_{13}$, i.e. 'tetrahedrite-(Cd)'. The former potential mineral phase was also described by Voropayev *et al.* (1988) from the Ushkatyn-III deposit, in central Kazakhstan. Their chemical analyses has Cd contents ranging between 0.93 and 0.99 apfu (recalculated on the basis of Σ*Me* = 16 apfu), Ag ≈ 3.1 apfu, and a Sb/(Sb+As) atomic ratio of 0.96. Dobbe (1992) reported electron microprobe data corresponding to composition varying between argentotetrahedrite-(Fe), 'argentotetrahedrite-(Mn)', and 'argentotetrahedrite-(Cd)'.

Škácha *et al.* (2016) described 'hakite' from Příbram, Central Bohemia (Czech Republic), and stressed the occurrence of different compositions characterised by the dominance of Hg^{2+}, Zn^{2+}, or Cd^{2+}. They indicated these different compositions as 'Hg-hakite', 'Zn-hakite', and 'Cd-hakite', ideally $Cu_6(Cu_4Hg_2)Sb_4Se_{13}$, $Cu_6(Cu_4Zn_2)Sb_4Se_{13}$ and $Cu_6(Cu_4Cd_2)Sb_4Se_{13}$, respectively. The crystal structure of 'Hg-hakite' was solved through electron diffraction tomography, confirming the isotypic relations with tetrahedrite and the occurrence of Hg^{2+} at the *M*(1) site.

Conclusion

Tennantite-(Cd) is a new member of the tetrahedrite group, further showing the role of these sulfosalts in hosting several transition elements typically occurring in hydrothermal environments. The recent revision of the nomenclature of the tetrahedrite group (Biagioni *et al.*, 2020a), approved by the International Mineralogical Association Commission on New Minerals, Nomenclature and Classification (IMA–CNMNC), promoted several studies on these sulfosalts, with the description of many different new mineral species and an increasing understanding of their crystal chemistry. The new life of this important sulfosalt group has implications in both the environmental and technological fields. Indeed, tetrahedrite-group minerals host not only economically valuable metals but also some environmentally significant species, e.g. As, Sb, Hg and Cd, and some recent studies focused on the weathering of these minerals and the fate of the potentially toxic elements (e.g. Majzlan *et al.*, 2018; Keim *et al.*, 2018). Moreover, the improved knowledge of their crystal chemistry is useful in evaluating the high-tech properties of these compounds (e.g. Chetty *et al.*, 2015; Levinsky *et al.*, 2019).

The description of tennantite-(Cd) shows both kinds of implications, owing to the presence of the toxic element Cd (e.g. Genchi *et al.*, 2020) as well as to its potential electronic properties, similar to those shown by its Sb-counterpart $Cu_{10}Cd_2Sb_4S_{13}$ (e.g. Kumar *et al*, 2016; Ghisani *et al.*, 2022).

Finally, the identification of the Cd-member of the tennantite series in the Berenguela mining district suggests that the re-examination of tetrahedrite-group mineral samples from this area could be interesting, improving our knowledge on the crystal chemistry of Cd-rich members of this sulfosalt group.

Acknowledgements. CB acknowledges financial support from the Ministero dell'Istruzione, dell'Università e della Ricerca through the project PRIN 2017 "TEOREM – deciphering geological processes using Terrestrial and Extraterrestrial ORE Minerals", prot. 2017AK8C32. The study was also financially supported by the Ministry of Culture of the Czech Republic (long-term project DKRVO 2019-2023/1.II.d; National Museum, 00023272) for JS. The comments of Peter Leverett, Yves Moëlo, and an anonymous reviewer improved the original manuscript.

Supplementary material. To view supplementary material for this article, please visit https://doi.org/10.1180/mgm.2022.61

Competing interests. The authors declare none.

References

Allen F.H., Bergerhoff G. and Sievers R. (1987) *Crystallographic Databases*. International Union of Crystallography, Chester, England (UK), 221 p.

Andreasen J.W., Makovicky E., Lebech B. and Karup-Møller S. (2008) The role of iron in tetrahedrite and tennantite determined by Rietveld refinement of neutron powder diffraction data. *Physics and Chemistry of Minerals*, **35**, 447–454.

Biagioni C., Bonaccorsi E., Moëlo Y., Orlandi P., Bindi L., D'Orazio M. and Vezzoni S. (2014) Mercury-arsenic sulfosalts from the Apuan Alps (Tuscany, Italy). II. Arsiccioite, $AgHg_2TlAs_2S_6$, a new mineral from the Monte Arsiccio mine: occurrence, crystal structure and crystal chemistry of the routhierite isotypic series. *Mineralogical Magazine*, **78**, 101–117.

Biagioni C., George L.L., Cook N.J., Makovicky E., Moëlo Y., Pasero M., Sejkora J., Stanley C.J., Welch M.D. and Bosi F. (2020a) The tetrahedrite group: Nomenclature and classification. *American Mineralogist*, **105**, 109–122.

Biagioni C., Sejkora J., Musetti S., Velebil D. and Pasero M. (2020b) Tetrahedrite-(Hg), a new 'old' member of the tetrahedrite group. *Mineralogical Magazine*, **84**, 584–592.

Biagioni C., Sejkora J., Raber T., Roth P., Moëlo Y., Dolníček Z. and Pasero M. (2021) Tennantite-(Hg), $Cu_6(Cu_4Hg_2)As_4S_{13}$, a new tetrahedrite-group mineral from the Lengenbach quarry, Binn, Switzerland. *Mineralogical Magazine*, **85**, 744–751.

Biagioni C., Sejkora J., Moëlo Y., Marcoux E., Mauro D. and Dolníček Z. (2022a) Tennantite-(Cu), $Cu_{12}As_4S_{13}$, from Layo, Arequipa Department, Peru: a new addition to the tetrahedrite-group minerals. *Mineralogical Magazine*, **86**, 331–339.

Biagioni, C., Kasatkin, A.V., Sejkora, J., Nestola, F. and Škoda, R. (2022b) Tennantite-(Cd), IMA 2021-083. CNMNC Newsletter 65. *Mineralogical Magazine*, **86**, 354–358.

Borsari M. (2014) Cadmium: coordination chemistry. In: *Encyclopedia of Inorganic and Bioinorganic Chemistry* (R.A. Scott, editor). https://doi.org/10.1002/9781119951438.eibc2261

Brese N.E. and O'Keeffe M. (1991) Bond-valence parameters for solids. *Acta Crystallographica*, **B47**, 192–197.

Burnham C.W. (1962) Lattice constant refinement. *Carnegie Institute Washington Yearbook*, **61**, 132–135.

Charlat M. and Lévy C. (1975) Influence des principales substitutions sur le parametre cristallin de la série tennantite-tétraédrite. *Bulletin de la Société Française de Mineralogie et de Cristallographie*, **98**, 152–158.

Charnock J.M., Garner C.D., Pattrick R.A.D. and Vaughan D.J. (1989) Coordination sites of metals in tetrahedrite minerals determined by EXAFS. *Journal of Solid State Chemistry*, **82**, 279–289.

Chetty R., Bali A. and Mallik R.C. (2015) Tetrahedrites as thermoelectric materials: an overview. *Journal of Material Chemistry C*, **3**, 12364–12378.

Criddle A.J. and Stanley C.J. (1993) *Quantitative Data File for Ore Minerals*, 3rd edition. Chapman & Hall, London.

Dobbe R.T.M. (1992) Manganoan-cadmian tetrahedrite from the Tunaberg Cu-Co deposit, Bergslagen, central Sweden. *Mineralogical Magazine*, **56**, 113–115.

Flack H.D. (1983) On enantiomorph-polarity estimation. *Acta Crystallographica*, **A39**, 876–881.

Genchi G., Sinicropi M.S., Lauria G., Carocci A. and Catalano A. (2020) The effects of cadmium toxicity. *International Journal of Environmental Research and Public Health*, **17**, 3782.

George L.L., Cook N.J. and Ciobanu C.L. (2017) Minor and trace elements in natural tetrahedrite-tennantite: effects on element partitioning among base metal sulphides. *Minerals*, **7**, 17.

Ghisani F., Timmo K., Altosaar M., Mikli V., Danilson M., Grossberg M. and Kauk-Kuusik M. (2022) Chemical etching of tetrahedrite $Cu_{10}Cd_2Sb_4S_{13}$ monograin powder materials for solar cell applications. *Materials Science in Semiconductor Processing*, **138**, 106291.

Jia D., Fu Z., Zhang H. and Zhao C. (1988) The first discovery of Cd-freibergite in China. *Acta Mineralogica Sinica*, **8**, 136–137.

Jimenez Ch., N., Barrera L., Flores O., Lizeca J.L., Murillo F., Sanjines O., Hardyman R.F., Tosdal R.M. and Wallace A.R. (1993) Magmatic evolution of the Berenguela-Charaña Northwestern Altiplano, Bolivia. *Second ISAG, Oxford* (*UK*), 377–380.

Johnson N.E. (1991) X-ray powder diffraction data for synthetic varieties of tetrahedrite. *Powder Diffraction*, **6**, 43–47.

Johnson M.L. and Burnham C.W. (1985) Crystal structure refinement of an arsenic-bearing argentian tetrahedrite. *American Mineralogist*, **70**, 165–170.

Johnson N.E., Craig J.R. and Rimstidt J.D. (1986) Compositional trends in tetrahedrite. *The Canadian Mineralogist*, **24**, 385–397.

Johnson N.E., Craig J.R. and Rimstidt J.D. (1987) Effect of substitutions on the cell dimensions of tetrahedrite. *The Canadian Mineralogist*, **25**, 237–244.

Johnson N.E., Craig J.R. and Rimstidt J.D. (1988) Crystal chemistry of tetrahedrite. *American Mineralogist*, **73**, 389–397.

Keim M.F., Staude S., Marquardt K., Bachmann K., Opitz J. and Markl G. (2018) Weathering of Bi-bearing tennantite. *Chemical Geology*, **499**, 1–25.

Kraus W. and Nolze G. (1996) POWDER CELL – a program for the representation and manipulation of crystal structures and calculation of the resulting X-ray powder patterns. *Journal of Applied Crystallography*, **29**, 301–303.

Kumar D.S.P., Chetty R., Rogl P., Rogl G., Bauer E., Malar P. and Mallik R.C. (2016) Thermoelectric properties of Cd doped tetrahedrite: $Cu_{12-x}Cd_xSb_4S_{13}$. *Intermetallics*, **78**, 21–29.

Levinsky P., Candolfi C., Dauscher A., Tobola A., Hejtmánek J. and Lenoir B. (2019) Thermoelectric properties of the tetrahedrite – tennantite solid solutions $Cu_{12}Sb_{4-x}As_xS_{13}$ and $Cu_{10}Co_2Sb_{4-y}As_yS_{13}$ $(0 \leq x,y \leq 4)$. *Physical Chemistry Chemical Physics*, **21**, 4547–4555.

Majzlan J., Kiefer S., Herrmann J., Števko M., Sejkora J., Chovan M., Lánczos T., Lazarov M., Gerdes A., Langenhorst F., Borčinová Radková A., Jamieson H. and Milovský R. (2018) Synergies in elemental mobility during weathering of tetrahedrite $[(Cu,Fe,Zn)_{12}(Sb,As)_4S_{13}]$: Field observations, electron microscopy, isotopes of Cu, C, O, radiometric dating, and water geochemistry. *Chemical Geology*, **488**, 1–20.

Makovicky E., Tippelt G., Forcher K., Lottermoser W., Karup-Møller S. and Amthauer G. (2003) Mössbauer study of Fe-bearing synthetic tennantite. *The Canadian Mineralogist*, **41**, 1125–1134.

Makovicky E., Karanović L., Poleti D., Balić-Žunić T. and Paar W.H. (2005) Crystal structure of copper-rich unsubstitued tennantite, $Cu_{12.5}As_4S_{13}$. *The Canadian Mineralogist*, **43**, 679–688.

Ondruš P. (1993) A computer program for analysis of X-ray powder diffraction patterns. *Materials Science Forum* (*EPDIC-2, Enchede*), **133–136**, 297–300.

Pattrick R.A.D. (1978) Microprobe analyses of cadmium-rich tetrahedrites from Tyndrum, Perthshire, Scotland. *Mineralogical Magazine*, **42**, 286–288.

Pattrick R.A.D. and Hall A.J. (1983) Silver substitution into synthetic zinc, cadmium, and iron tetrahedrites. *Mineralogical Magazine*, **47**, 441–451.

Pouchou J.L., and Pichoir F. (1985) "PAP" (φρZ) procedure for improved quantitative microanalysis. Pp. 104–106 in: *Microbeam Analysis* (J.T. Armstrong, editor). San Francisco Press, San Francisco.

Sheldrick G.M. (2015) Crystal Structure Refinement with SHELXL. *Acta Crystallographica*, **C71**, 3–8.

Škácha P., Sejkora J., Palatinus L., Makovicky E., Plášil J., Macek I. and Goliáš V. (2016) Hakite from Příbram, Czech Republic: compositional variability, crystal structure and the role in Se mineralization. *Mineralogical Magazine*, **80**, 1115–1128.

Skinner B.J. (1961) Unit-cell edges of natural and synthetic sphalerites. *American Mineralogist*, **46**, 1399–1411.

Spiridonov E.M., Petrov V.K. and Voropayev A.V. (1988) Effect of cadmium on the optical properties of fahlore minerals. *Transactions of the USSR Academy of Sciences, Earth Science Sections*, **303**, 134–137 [in Russian].

Voropayev V.K., Spiridonov E.M., and Shchibrik V.I. (1988) Cd-tetrahedrite, first find in the USSR. *Transactions of the USSR Academy of Sciences, Earth Science Sections*, **300**, 131–133.

Voudouris P.C., Spry P.G., Sakellaris G.A. and Mavrogonatos C. (2011) A cervelleite-like mineral and other Ag-Cu-Te-S minerals [Ag_2CuTeS and $(Ag,Cu)_2TeS$] in gold-bearing veins in metamorphic rocks of the Cycladic Blueschist Unit, Kallianou, Evia Island, Greece. *Mineralogy and Petrology*, **101**, 169–183.

Wallace A.R. (1975) Berenguela district. Pp 129–131 in: *Geology and Mineral Resources of the Altiplano and Cordillera Occidental, Bolivia*. U.S. Geological Survey Bulletin, Colorado, USA.

Wang Y., Chen R., Gu X., Yang Z., Hou Z., Fan G., Ye L. and Qu K. (2021) Tennantite-(Ni), IMA 2021-018. CNMNC Newsletter 62. *Mineralogical Magazine*, **85**, 634–638.

Warr L.N. (2021) IMA-CNMNC approved mineral symbols. *Mineralogical Magazine*, **85**, 291–320.

Wedepohl K.H. (1995) The composition of the continental crust. *Geochimica et Cosmochimica Acta*, **59**, 1217–1232.

Welch M.D., Stanley C.J., Spratt J. and Mills S.J. (2018) Rozhdestvenskayaite $Ag_{10}Zn_2Sb_4S_{13}$ and argentotetrahedrite $Ag_6Cu_4(Fe^{2+},Zn)_2Sb_4S_{13}$: two Ag-dominant members of the tetrahedrite group. *European Journal of Mineralogy*, **30**, 1163–1172.

Wilson A.J.C. (1992) *International Tables for Crystallography*. Volume C. Kluwer, Dordrecht, The Netherlands.

Wuensch B.J. (1964) The crystal structure of tetrahedrite, $Cu_{12}Sb_4S_{13}$. *Zeitschrift für Kristallographie*, **119**, 437–453.

Wuensch B.J., Takéuchi Y. and Nowacki W. (1966) Refinement of the crystal structure of binnite, $Cu_{12}As_4S_{13}$. *Zeitschrift für Kristallographie*, **123**, 1–20.

Xu Y.N. and Ching W.Y. (1993) Electronic, optical, and structural properties of some wurtzite crystals. *Physical Reviews*, **B48**, 4335–4351.

https://doi.org/10.1180/mgm.2022.61 Published online by Cambridge University Press